

# Electric-field controlled nonlinear anomalous Nernst effect in two-dimensional time-reversal symmetric systems

Ying-Li Wu<sup>1</sup> and Xiao-Qin Yu<sup>1\*</sup>

<sup>1</sup> School of Physics and Electronics, Hunan University, Changsha 410082, China

It's established that the nonlinear anomalous Nernst effect (NANE), originating from Berry curvature near the Fermi energy, is symmetry-permitted only when a single mirror symmetry exists in the transport plane of two-dimensional (2D) materials. Here, we show that an applied direct electric field can lift this symmetry constraint, enabling an electric-field-induced NANE emerge in time-reversal symmetric 2D systems with higher crystallographic symmetries. This electric-field-induced NANE arises from both Berry connection polarization, rooted in the electric-field-corrected Berry curvature, and the anomalous-velocity-modified nonequilibrium Fermi distribution function. Additionally, we propose an alternating temperature gradient as a driving force instead of the conventional steady one, ensuring experimental detection of NANE via second-harmonic measurement techniques. The behaviour of electric-field-induced NANE in the monolayer graphene has been theoretically and systematically investigated.

## I. INTRODUCTION

The Hall (Nernst) effects, referring to a generation of transverse current in response to a longitudinal electric field (temperature gradient), represent important paradigms in condensed matter physics<sup>1–3</sup>. Traditionally, Hall effects (e.g., conventional, anomalous, and thermal Hall effects) were believed to require broken time-reversal ( $\mathcal{T}$ ) symmetry. However, the 2015 discovery of the nonlinear anomalous Hall effect (NAHE)<sup>4</sup>, a second-harmonic response to an alternating electric field, in  $\mathcal{T}$ -symmetric but inversion ( $\mathcal{P}$ ) symmetric broken systems reveals that Hall voltage can emerge in the  $\mathcal{T}$ -symmetric systems, reshaping our understanding that Hall responses require the  $\mathcal{T}$  symmetry breaking. NAHE originates from the Berry curvature dipole (BCD)<sup>4–11</sup>, a first-order moment of the Berry curvature over the occupied states in momentum space, instead of Berry curvature (BC), attracting broad interests in exploration of the nonlinear transport phenomena stemming from other quantum geometric beyond BC. A series of novel nonlinear transport phenomena are identified, such as nonreciprocal magnetoresistance (NMTR)<sup>12,13</sup>, intrinsic planar Hall effect (IPHE)<sup>14,15</sup>, nonlinear thermal Hall effect<sup>16–20</sup>, and nonlinear anomalous Nernst effect (NANE)<sup>20–25</sup>.

NANE<sup>21–23</sup>, a nonlinear thermoelectric phenomenon in second-order response to the temperature gradient, originates from BC near the Fermi energy and has a quantum origin rooted in a pseudotensorial quantity  $\Lambda_{cd}^T = -\int[d\mathbf{k}]\Omega_c(\mathbf{k})\partial_{k_d}f_0(\varepsilon_{\mathbf{k}} - E_f)^2/T^2$ , which is analogous to the BCD, where  $f_0$  is the equilibrium Fermi distribution function,  $\varepsilon_{\mathbf{k}}$  represents energy band, and  $E_f$  indicates Fermi energy. Like BCD-induced NAHE, this NANE exhibits a linear dependence on relaxation time  $\tau$  and also does not require  $\mathcal{T}$  symmetry breaking instead relies on  $\mathcal{P}$  symmetry breaking. In addition, the largest symmetry for nonvanishing NANE in the transport plane of the two-dimensional (2D) materials is a single mirror line<sup>21–23</sup>.

Beyond the  $\tau$ -linearly-dependent NANE originating

from quantity  $\Lambda^T$ , an intrinsic  $\tau$ -independent NANE can also emerge in  $\mathcal{PT}$ -symmetric systems arising from either the orbital magnetic quadrupole moment<sup>26</sup> or thermal Berry connection polarizability<sup>20</sup>. Being analogous to the linear Nernst effect, however, the intrinsic NANE disappears in the presence of  $\mathcal{T}$  symmetry. Consequently, both intrinsic and  $\Lambda^T$ -induced inherent NANE are suppressed in the  $\mathcal{T}$ -symmetric 2D materials with high crystal symmetries (e.g., those with symmetries higher than a single mirror line in the transport plane), which severely restricts the selection range of materials for the NANE.

Recently, it's been reported that the symmetry constraint on the BCD-induced NAHE can be lifted via electric-field engineering<sup>27–32</sup>, wherein an additional dc electric field  $\mathbf{E}^{dc}$  applied to the NAHE experimental setup induces a field-induced BCD correction, which is proportional to the Berry connection polarization (BCP)<sup>27–31,33</sup>. Importantly, studies reveal that the field-induced BCD can exist in systems where the inherent BCD and BC are symmetry-forbidden, including 1)  $\mathcal{T}$ -symmetric 2D materials with crystal symmetries beyond single mirror symmetry (e.g., dual mirror Rashba systems<sup>28</sup> and  $C_2$ -symmetric  $p$ -wave antiferromagnets<sup>30</sup>); and 2)  $\mathcal{T}$  symmetry-broken materials, such as  $g$ -wave altermagnet with four-fold rotation symmetry ( $C_4$ )<sup>30</sup> and  $d$ -wave altermagnet with combined  $C_4\mathcal{T}$  symmetry<sup>29,30</sup>. Consequently, a second-harmonic Hall voltage can be generated from the field-induced BCD in the systems, where the inherent-BCD-induced NAHE is symmetry-suppressed. Experimentally, the field-induced BCD and its associated NAHE have been observed in thick  $T_d$ -WTe<sub>2</sub> with effective  $\mathcal{P}$  symmetry in the  $x$ - $y$  plane<sup>27</sup>.

In this paper, we theoretically investigate the electric-field-induced NANE as a second-harmonic response to an *alternating* temperature gradient  $\nabla T^\omega(t) = \text{Re}\{\tilde{\nabla}T e^{i\omega t}\}$  (where  $\tilde{\nabla}T \in \mathcal{C}$  is the spatially uniform complex amplitude vector of  $\nabla T^\omega$ , and  $\omega$  indicates frequency) [Fig. 1] and analyze the crystal symmetry constraint on this NANE in the  $\mathcal{T}$ -symmetric 2D materials. In previous theoretical studies on NANE or other

thermally driven thermoelectric phenomena, researchers typically consider a steady (time-independent) dc temperature gradient  $\nabla T^{\text{dc}}$  and investigate the dc response, as the experimental realization of  $\nabla T^\omega$  is challenging. However, a regulatable  $\nabla T^\omega$  has recently been realized experimentally by passing an alternating current  $I_h^{\omega/2} = I_0 \sin(\omega t/2 + \phi_0)$  to a microheater electrode<sup>25</sup>. The use of alternating temperature gradients in electric-field-induced NANE allows exclusion of spurious nonlinear currents (e.g., second-order in  $\mathbf{E}^{\text{dc}}$  and first-order in  $\text{Re}\{\tilde{\nabla}T\}$ ) through measuring the second-harmonic voltage via lock-in amplification.

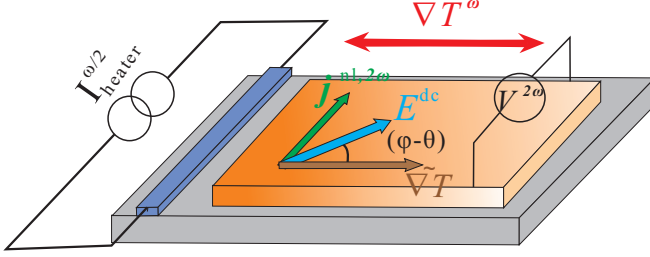


FIG. 1. Schematic of the measurement setup for electric-field-induced NANE, showing the complex amplitude vector  $\tilde{\nabla}T$  of the alternating temperature gradient  $\nabla T^\omega$  and direct electric field  $\mathbf{E}^{\text{dc}}$  in the same plane.  $\nabla T^\omega$  is generated by passing an alternating current  $I_{\text{heater}}^{\omega/2}$  with frequency  $\omega/2$  to a microheater electrode.  $\theta$  ( $\varphi$ ) represents the polar angle of  $\tilde{\nabla}T$  ( $\mathbf{E}^{\text{dc}}$ ) with respect to  $x$ -axis, which is taken as a crystal axis (e.g. the zigzag direction in graphene).

The paper is organized as follows. We firstly review the  $\Lambda^T$ -induced inherent NANE driven by a steady temperature gradient, and then derive the formula of the rectified ( $j_a^{\text{nl},0}$ ) and second-harmonic ( $j_a^{\text{nl},2\omega}$ ) currents as a second response to the alternating  $\nabla T^\omega$  in the presence of  $\mathbf{E}^{\text{dc}}$  based on the Boltzmann theory in Sec. II. The symmetry constraints on the nonlinear anomalous Nernst coefficients (NANCs) are analyzed, and the angular dependence of electric-field-induced NANC  $\xi_{abcd}$  on the orientations of  $\mathbf{E}^{\text{dc}}$  and  $\nabla T^\omega$  with respect to the principal crystal axis is investigated in Sec. III. The behavior of the electric-field-induced NANE for the monolayer graphene is discussed in Sec. IV. Finally, we give a conclusion in Sec. V.

## II. THEORETICAL REVIEW AND DERIVATION

The relation between nonlinear anomalous Nernst current  $\mathbf{j}^{\text{nl}}$  (where the superscript “nl” refers to nonlinear) and the pseudotensorial quantity  $\Lambda_{cd}^T$  has been recently determined through the semiclassical framework of the electron dynamics<sup>21,22</sup>. We here briefly review the NANE in 2D systems, in which the BC transforms from a pseudovector to a pseudoscalar, with only the out-of-plane component ( $\Omega_c = z$ ) remaining nonzero. Consequently,

$\Lambda_{cd}^T$  exhibits pseudovector behavior confined to the 2D plane as

$$\Lambda^T = - \int [d\mathbf{k}] \frac{(\varepsilon_{\mathbf{k}} - E_f)^2}{T^2} \frac{\partial f_0}{\partial \mathbf{k}} \Omega_z(\mathbf{k}), \quad (1)$$

where  $\int [d\mathbf{k}]$  is the shorthand for  $\int d\mathbf{k}/(2\pi)^2$ ,  $\Omega_c(\mathbf{k}) = [\nabla_{\mathbf{k}} \times \mathbf{A}(\mathbf{k})]_c$  denotes the inherent BC, and  $\mathbf{A}(\mathbf{k}) = \langle u_n(\mathbf{k}) | i\nabla_{\mathbf{k}} | u_n(\mathbf{k}) \rangle$  denotes the intraband Berry connection with  $|u_n(\mathbf{k})\rangle$  being the periodic part of the Bloch wave-function for band  $n$ . In fact, the largest symmetry allowed for a nonvanishing  $\Lambda^T$  in the transport plane ( $x$ - $y$  plane) is a single mirror line (a mirror plane that is orthogonal to the 2D crystal)<sup>21</sup>. The nonlinear Nernst current  $\mathbf{j}^{\text{nl}}$  as a response to the second order in steady dc temperature gradient  $\nabla T^{\text{dc}}$  is

$$\mathbf{j}^{\text{nl}} = \frac{e\tau}{\hbar^2} (\hat{z} \times \nabla T^{\text{dc}}) (\nabla T^{\text{dc}} \cdot \Lambda^T), \quad (2)$$

where  $\hbar$  is the Planck constant, and  $\tau$  refers to relaxation time.

Within the extended semiclassical theory, it has been established that Berry connection experiences a gauge-invariant correction  $\mathcal{A}_a^E = \tilde{\mathcal{G}}_{ab}(\mathbf{k}) E_b^{\text{dc}}$  under an applied  $\mathbf{E}^{\text{dc}}$ ,<sup>34-37</sup> where  $\tilde{\mathcal{G}}_{ab}(\mathbf{k})$  represents the component of BCP tensor and is defined for the band  $n$  as:

$$\tilde{\mathcal{G}}_{ab}(\mathbf{k}) = 2e \text{Re} \sum_{m \neq n} \frac{\mathcal{A}_a^{nm}(\mathbf{k}) \mathcal{A}_b^{mn}(\mathbf{k})}{\varepsilon_{\mathbf{k}}^n - \varepsilon_{\mathbf{k}}^m}, \quad (3)$$

with  $\mathcal{A}_a^{nm}(\mathbf{k}) = \langle u_n(\mathbf{k}) | i\partial_{k_a} | u_m(\mathbf{k}) \rangle$  indicating the interband Berry connection. This gauge-invariant correction directly generates a field-induced BC  $\mathbf{\Omega}^E(\mathbf{k}) = \nabla \times \mathbf{A}^E(\mathbf{k})$ , a correction to the BC as  $\tilde{\mathbf{\Omega}}(\mathbf{k}) = \mathbf{\Omega}(\mathbf{k}) + \mathbf{\Omega}^E(\mathbf{k})$ , which can lead to a electric-field-induced NANE investigated as following.

Taking the Berry-phase correction to the orbital magnetization into consideration, the formula of charge transport current  $\mathbf{j}$  driven by the statistical force, arising from the temperature gradient  $\nabla T$ , has been derived through the semiclassical theory in previous works<sup>3,21</sup> and is given by

$$\mathbf{j} = -e \int [d\mathbf{k}] \dot{r} f - \frac{\nabla T}{T} \times \frac{e}{\hbar} \int [d\mathbf{k}] \tilde{\mathbf{\Omega}}(\mathbf{k}) [(\varepsilon_{\mathbf{k}} - \mu) f(\mathbf{k}) + k_B T \ln(1 + e^{-\frac{(\varepsilon_{\mathbf{k}} - \mu)}{k_B T}})], \quad (4)$$

where the first term is conventional current, and the second term is anomalous charge current stemming from the BC,  $f(\mathbf{k})$  represents the nonequilibrium distribution function (NDF), which was initially written as equilibrium distribution function  $f_0$  in the original work<sup>3</sup> but has been extended into the nonequilibrium situation by Yu *et al.*<sup>21</sup> Considering the effect of the electric-field-induced BC  $\mathbf{\Omega}^E(\mathbf{k})$ , we have replaced the inherent BC  $\mathbf{\Omega}(\mathbf{k})$  by the electric-field corrected BC  $\tilde{\mathbf{\Omega}}(\mathbf{k})$  in Eq. (4).

When in presence of  $\nabla T^\omega$  and  $\mathbf{E}^{\text{dc}}$  simultaneously,  $f(\mathbf{k})$  can be determined through solving the Boltzmann

TABLE I. Symmetry constraints on  $\xi_{abcd}^{\text{BCP/NDF-AV}}$  and  $\chi_{abc}$  tensors from point group symmetries pertaining to 2D time-reversal symmetric materials. '✓' ('✗') means the element is symmetry allowed (forbidden). Here,  $M_b$ ,  $C_n^b$ , and  $S_n^b$  represent mirror,  $n$ -fold rotation, and  $n$ -fold rotation-reflection symmetry operation along the  $b$  direction for  $b = \{x, y, z\}$ , respectively.

Elemental crystallographic symmetries							Point Groups			
$C_2^z$	$C_2^x$	$C_2^y$	$C_{3,4,6}^z$ $S_{4,6}^z$	$M_z$	$M_x$	$M_y$	$C_{1v}(\sigma_y)$	$C_{1v}(\sigma_x)$	$C_{2v}, D_2$	$C_{3v,4v,6v}, D_{3,4,6}$ $D_{2d}, D_{3h}$
$\xi_{xyyy}^{\text{BCP}}$	✓	✗	✗	✓	✓	✗	✗	✗	✗	✗
$\xi_{xyyx}^{\text{BCP/NDF-AV}}$	✓	✓	✓	✓	✓	✓	✓	✓	✓	✓
$\xi_{yxxx}^{\text{BCP}}$	✓	✗	✗	- $\xi_{xyyy}^{\text{BCP}}$	✓	✗	✗	✗	✗	✗
$\xi_{yxyy}^{\text{BCP/NDF-AV}}$	✓	✓	✓	$\xi_{xyyy}^{\text{BCP/NDF-AV}}$	✓	✓	✓	✓	✓	$\xi_{xyyx}^{\text{BCP/NDF-AV}}$
$\chi_{xyy}$	✗	✓	✗	✗	✓	✓	✓	✗	✗	✗
$\chi_{yxx}$	✗	✗	✓	✗	✓	✓	✗	✓	✗	✗

transport equation. We are interested in the response up to the second order in temperature gradient and first order in electric field, and hence have approximated NDF as  $f \approx \text{Re}\{f_0 + \delta f^{(1,0)} + \delta f^{(0,1)} + \delta f^{(1,1)} + \delta f^{(0,2)}\}$  with the high-order terms  $\delta f^{(n,m)}$  corresponding to  $n$ -th order in  $E^{\text{dc}}$  and  $m$ -th order in  $\text{Re}\{\partial_a T\}$  understood to vanish. After a series of careful derivation (see details in Appendix A), the formulas for expansion coefficients [ $\delta f^{(1,0)}$ ,  $\delta f^{(0,1)}$ ,  $\delta f^{(1,1)}$  and  $\delta f^{(0,2)}$ ] can be determined as

$$\begin{aligned} \delta f^{(1,0)} &= \frac{e\tau}{\hbar} \mathbf{E}^{\text{dc}} \cdot \nabla_{\mathbf{k}} f_0, & \delta f^{(0,1)} &= \delta f_{\omega}^{(0,1)} e^{i\omega t}, \\ \delta f^{(1,1)} &= \delta f_{\omega}^{(1,1)} e^{i\omega t}, & \delta f^{(0,2)} &= \delta f_0^{(0,2)} + \delta f_{2\omega}^{(0,2)} e^{2i\omega t}, \end{aligned} \quad (5)$$

where the amplitudes [ $\delta f_{\omega}^{(0,1)}$ ,  $\delta f_{\omega}^{(1,1)}$ ,  $\delta f_0^{(0,2)}$ , and  $\delta f_{2\omega}^{(0,2)}$ ] are given in Eq. (A12). Hence, the  $a$ -component of nonlinear anomalous Nernst current  $j_a^{\text{nl}}$  as second-order response to the temperature gradient can be written as (see the details in Appendix B)

$$j_a^{\text{nl}} = \text{Re}\{j_a^{\text{nl},0} + j_a^{\text{nl},2\omega} e^{2i\omega t}\}, \quad (6)$$

where  $j_a^{\text{nl},0}$  and  $j_a^{\text{nl},2\omega}$  represents the rectified and the second harmonic current, respectively, and can be written as

$$\begin{aligned} j_a^{\text{nl},0} &= (\chi_{abc} + \xi_{abcd} E_d^{\text{dc}}) (\partial_b \tilde{T})^* \partial_c \tilde{T}, \\ j_a^{\text{nl},2\omega} &= (\chi_{abc} + \xi_{abcd} E_d^{\text{dc}}) \partial_b \tilde{T} \partial_c \tilde{T}. \end{aligned} \quad (7)$$

After a series of careful derivation (details can be found in Appendix B), the explicit expressions for the inherent ( $\chi_{abc}$ ) and electric-field-induced ( $\xi_{abcd}$ ) NANCs have been systematically derived for both 2D and three-dimensional systems with  $\mathcal{T}$  symmetry. We focus exclusively on the 2D systems. The derived forms of  $\chi_{abc}$  and  $\xi_{abcd}$  in  $\mathcal{T}$ -symmetric 2D systems are given by

$$\begin{aligned} \chi_{abc} &= \frac{\tau e \epsilon_{abz}}{2(1+i\omega\tau)\hbar^2} \Lambda_c^T, & \xi_{abcd} &= \xi_{abcd}^{\text{BCP}} + \xi_{abcd}^{\text{NDF-AV}}, \\ \xi_{abcd}^{\text{BCP}} &= \frac{\tau e \epsilon_{abz}}{2(1+i\omega\tau)\hbar^2} \Upsilon_{cd}, & \xi_{abcd}^{\text{NDF-AV}} &= \frac{\tau e^2 \epsilon_{abz} \epsilon_{cdz}}{2(1+i\omega\tau)\hbar^2} \Gamma, \end{aligned} \quad (8)$$

where the superscript "AV" refer to anomalous velocity,  $\epsilon_{abz}$  represents the Levi-Civita symbol, and pseudotensorial (scalar) quantity  $\Upsilon_{cd}(\Gamma)$  is defined as

$$\begin{aligned} \Upsilon_{cd} &= \int [d\mathbf{k}] \left[ \frac{\partial \tilde{\mathcal{G}}_{xd}(\mathbf{k})}{\partial k_y} - \frac{\partial \tilde{\mathcal{G}}_{yd}(\mathbf{k})}{\partial k_x} \right] \frac{(\varepsilon_{\mathbf{k}} - E_f)^2}{T^2} \frac{\partial f_0}{\partial k_c}, \\ \Gamma &= - \int [d\mathbf{k}] \Omega_z^2(\mathbf{k}) \frac{(\varepsilon_{\mathbf{k}} - E_f)^2}{T^2} \frac{\partial f_0}{\partial \varepsilon_{\mathbf{k}}}. \end{aligned} \quad (9)$$

The components  $\xi_{abcd}^{\text{BCP}}$  and  $\xi_{abcd}^{\text{NDF-AV}}$  stem from BCP and the corrected NDF [Eq. (A8)] induced by anomalous velocity  $(\mathbf{E} \times \boldsymbol{\Omega})$ , respectively. The BCP contribution roots in the electric-field-induced BC. In this work, we focus on the second-harmonic response, which can be measured via lock-in amplification. Hence, only  $j_a^{\text{nl},2\omega}$  will be investigated in subsequent analysis. In vector notation, the second harmonic current  $\mathbf{j}^{\text{nl},2\omega}$  can be further written as

$$\begin{aligned} \mathbf{j}^{\text{nl},2\omega} &= \frac{e\tau}{2(1+i\omega\tau)\hbar^2} (\hat{z} \times \tilde{\nabla} T) (\tilde{\nabla} T \cdot \Lambda^T) \\ &+ \frac{e\tau}{2(1+i\omega\tau)\hbar^2} (\hat{z} \times \tilde{\nabla} T) (\tilde{\nabla} T \cdot \overleftrightarrow{\Upsilon}) \cdot \mathbf{E}^{\text{dc}} \quad (10) \\ &+ \frac{e^2 \tau \Gamma}{(1+i\omega\tau)\hbar^2} (\hat{z} \times \tilde{\nabla} T) (\hat{z} \times \tilde{\nabla} T) \cdot \mathbf{E}^{\text{dc}}, \end{aligned}$$

showing the current  $\mathbf{j}^{\text{nl},2\omega}$  corresponds to Nernst current, as  $\mathbf{j}^{\text{nl},2\omega} \cdot \tilde{\nabla} T = 0$ . When  $\mathbf{E}^{\text{dc}} \parallel \tilde{\nabla} T$ , the third terms originating from  $\xi_{abcd}^{\text{NDF-AV}}$  in Eq. (10) becomes zero, indicating that the contribution from the anomalous-velocity-modified NDF vanishes, and the electric-field-induced NANE solely stems from the BCP.

### III. SYMMETRIES ANALYSIS AND ANGULAR DEPENDENCY

Equation (8) implies both the rank-three tensor  $\chi_{abc}$  and the rank-four tensor  $\chi_{abcd}$  are antisymmetric in  $a$  and  $b$ , namely  $\chi_{abc} = -\chi_{bac}$  and  $\xi_{abcd} = -\xi_{bacd}$ . This antisymmetry implies all components with  $a = b$  are zero since  $\chi_{aac} = -\chi_{aac}$  and  $\xi_{aacd} = -\xi_{aacd}$ . As a result,

there are at most two (four) independent tensor elements for  $\chi$  ( $\xi$ ) in the 2D systems, which we choose here as  $[\chi_{xyy}, \chi_{yxx}]$  and  $[\xi_{xyyx}, \xi_{xyyy}, \xi_{yxxx}, \xi_{yxyy}]$ . Furthermore, we note  $\xi_{xyyy}^{\text{NDF-AV}} = 0$  and  $\xi_{yxxx}^{\text{NDF-AV}} = 0$  since the contribution from the anomalous-velocity-modified NDF to  $j^{\text{nl},2\omega}$  [i.e., the third term in Eq. (10)] vanishes when  $\mathbf{E}^{\text{dc}} \parallel \nabla T$ .

Further constraints on the coefficients  $[\chi_{abc}$ , and  $\xi_{abcd}]$  come from the crystalline point-group symmetries including  $\mathcal{P}$  symmetry. Under  $\mathcal{P}$  symmetry, the current  $j^{\text{nl}}$  changes sign but  $\partial_b T \partial_c T$  remains unchanged, restricting  $\chi_{abc}$   $\mathcal{P}$ -odd ( $\chi_{abc} \xrightarrow{\mathcal{P}} -\chi_{abc}$ ). This  $\mathcal{P}$ -odd parity forces  $\chi_{abc}$  to vanish in the systems with  $\mathcal{P}$  symmetry. However, the  $d$ -component of dc electric field  $E_d^{\text{dc}}$  [Eq. (7)] also changes sign under  $\mathcal{P}$  symmetry, resulting in  $\xi_{abcd}$   $\mathcal{P}$ -even ( $\xi_{abcd} \xrightarrow{\mathcal{P}} \xi_{abcd}$ ). The coefficient  $\xi_{abcd}$  has been decomposed into two parts as  $\xi_{abcd} = \xi_{abcd}^{\text{BCP}} + \xi_{abcd}^{\text{NDF-AV}}$  [Eq. (8)], and one can further confirm  $\xi_{abcd}^{\text{NDF-AV}} = 0$  in presence of both  $\mathcal{T}$  and  $\mathcal{P}$  symmetries. That's because BC satisfies  $\Omega(\mathbf{k}) = -\Omega(-\mathbf{k})$  under  $\mathcal{T}$  symmetry and  $\Omega(\mathbf{k}) = \Omega(-\mathbf{k})$  under  $\mathcal{P}$  symmetry, resulting in  $\Omega(\mathbf{k}) = 0$  at each point in the momentum space when both  $\mathcal{T}$  and  $\mathcal{P}$  symmetries are present. Be different to the BC, BCP  $\tilde{\mathcal{G}}(\mathbf{k})$  can exist in the presence of both  $\mathcal{P}$  and  $\mathcal{T}$  symmetries since the sign of  $\tilde{\mathcal{G}}(\mathbf{k})$  remains unchange under  $\mathcal{T}/\mathcal{P}$  symmetries, namely  $\tilde{\mathcal{G}}(\mathbf{k}) \xrightarrow{\mathcal{P}/\mathcal{T}} \tilde{\mathcal{G}}(-\mathbf{k})$ . Consequently, a nonlinear Nernst current can also emerge in the systems with both  $\mathcal{T}$  and  $\mathcal{P}$  symmetries, which attributes to the nonzero electric-field-induced NANC from BCP.

In addition to  $\mathcal{T}$  and  $\mathcal{P}$  symmetries, the constraint imposed by other crystal symmetry operations  $\mathcal{R}$  can be expressed as:

$$\begin{aligned} \chi_{abc} &= \mathcal{R}_{aa'} \mathcal{R}_{bb'} \mathcal{R}_{cc'} \chi_{a'b'c'}, \\ \xi_{abcd} &= \mathcal{R}_{aa'} \mathcal{R}_{bb'} \mathcal{R}_{cc'} \mathcal{R}_{dd'} \xi_{a'b'c'd'}, \end{aligned} \quad (11)$$

where  $\mathcal{R}$  represents a point group operation. The obtained symmetry constraints on the independent coefficients  $[\chi_{xyy}, \chi_{yxx}, \xi_{xyyx}^{\text{NDF-AV}}, \xi_{xyyy}^{\text{NDF-AV}}, \xi_{xyyx}^{\text{BCP}}, \xi_{xyyy}^{\text{BCP}}, \xi_{yxxx}^{\text{BCP}}, \xi_{yxyy}^{\text{BCP}}]$  for 2D case are summarized in Table I. In addition to the symmetry operations confined to the transport plane ( $x$ - $y$  plane), including  $n$ -th fold rotational symmetries  $C_n^z$  ( $n = 2, 3, 4, 6$ ) around  $z$  axis, and the vertical mirror symmetries  $M_a$  ( $a = x$  or  $y$ ), we have also analyse three kinds of out-of-plane symmetry operations involving the inversion ( $\mathcal{R}z = -z$ ), namely twofold rotation symmetries  $C_2^a$  around  $a$  axis, a horizontal mirror symmetry  $M_z$ , and rotation-reflection symmetry  $S_{4,6}^z$ , as they are permissible in certain layered 2D crystal materials. The inherent NANE from  $\Lambda^T$  are permitted in out-of-plane symmetries  $C_2^a$  and  $M_z$ . Obviously, the applied  $\mathbf{E}^{\text{dc}}$  removes the symmetry constraint on the NANE, specifically eliminating the requirement that the largest symmetry allowing  $\chi_{aa\perp a\perp} \neq 0$  in the transport plane is the single mirror symmetry  $M_{a\perp}$  ( $a\perp$  indicates axis perpendicular to  $a = \{x$  or  $y\}$

axis in 2D plane)<sup>21</sup>. All the independent NANCs  $[\xi_{xyyx}^{\text{NDF-AV}}, \xi_{xyxy}^{\text{NDF-AV}}, \xi_{yxxx}^{\text{BCP}}, \xi_{xyyy}^{\text{BCP}}, \xi_{yxxx}^{\text{BCP}}, \xi_{yxyy}^{\text{BCP}}]$  controlled by electric field are permitted in  $C_2^z$ -symmetric systems (the effective  $\mathcal{P}$  symmetry in the transport plane). When  $\mathbf{E}^{\text{dc}} \perp \nabla T^\omega$ , the coefficients  $\xi_{aa\perp a\perp a}^{\text{NDF-AV/BCP}}$ , are allowed across all elemental crystallographic symmetries applicable to 2D systems [Table. I]. Conversely, for  $\mathbf{E}^{\text{dc}} \parallel \nabla T^\omega$ , the term  $\xi_{aa\perp a\perp a\perp}^{\text{BCP}}$  are only permitted for symmetries  $[C_{n=2,3,4,6}^z, S_{4,6}^z \text{ and } M_z]$  but forbidden by  $C_2^{x,y}$  and  $M_{x,y}$  symmetries.

For the most Nernst transport experiments, the setup has a planar geometry, where the temperature gradient and the generated current are both within the plane (labeled as the  $x$ - $y$  plane). In this work, we further assume the  $\mathbf{E}^{\text{dc}}$ , which was applied to control the NANE, coplanar with  $\nabla T^\omega$ . In general,  $\nabla T^\omega$  and  $\mathbf{E}^{\text{dc}}$  are not aligned with the crystal axis but orients in a polar angle with respect to the  $x$ -direction (having taken to be a crystal direction), i.e.,  $(\partial_x T, \partial_y T) = \tilde{\partial}T(\cos \theta, \sin \theta)$  and  $(E_x, E_y) = E(\cos \varphi, \sin \varphi)$ , where  $\tilde{\partial}T = [(\partial_x T)^2 + (\partial_y T)^2]^{1/2}$ . Then, the electric-field-induced nonlinear second-harmonic Nernst current  $j_N^{\text{nl},2\omega}$  (where the subscript “N” represents the Nernst), flowing perpendicularly to the temperature gradient  $\nabla T^\omega$ , can be expressed as

$$j_N^{\text{nl},2\omega} = \xi_N(\theta, \varphi) \tilde{\partial}T \tilde{\partial}TE, \quad (12)$$

with the angle-dependent scalar coefficient  $\xi_N(\theta, \varphi)$  determined by the combination of the  $\xi$  tensor elements as (see Appendix C for a detail discussion)

$$\begin{aligned} \xi_N(\theta, \varphi) &= (\xi_{yxxx}^{\text{BCP}} \cos \varphi + \xi_{yxyy}^{\text{BCP}} \sin \varphi) \cos \theta \\ &\quad - (\xi_{xyyx}^{\text{BCP}} \cos \varphi + \xi_{xyyy}^{\text{BCP}} \sin \varphi) \sin \theta, \end{aligned} \quad (13)$$

where  $\xi_{abcd} = \xi_{abcd}^{\text{NDF-AV}} + \xi_{abcd}^{\text{BCP}}$  with  $\xi_{yxxx}^{\text{NDF-AV}} = \xi_{xyyy}^{\text{NDF-AV}} = 0$  (see details in Sec. III). Under the symmetry constraints outlined in Table I for the tensor components  $\xi_{abcd}$ , the angular dependence of the electric-field-induced NANE response becomes richer and more interesting. For example, the angular dependence of the electric-field-induced NANC reduces to

$$\xi_N(\theta, \varphi) = (\xi_{yxyy}^{\text{BCP}} + \xi_{xyyx}^{\text{NDF-AV}}) \sin(\varphi - \theta) \quad (14)$$

for the chiral groups  $C_{nv}$  and dihedral groups  $D_n$  ( $n > 2$ ), since they support only one independent tensor element  $\xi_{xyyx} = \xi_{yxyy}$  [Table. I].

Equation (13) shows that the electric-field-induced NANE can originate from both BCP contribution and anomalous-velocity-modified NDF contribution. However, the contribution from the anomalous-velocity-modified NDF [ $\xi^{\text{NDF-AV}}$ ] can be actually eliminated by aligning the electric field and temperature gradient along  $\pm x$  or  $\pm y$  axis. This exclusion is achieved through two configurations: 1) Parallel alignment ( $\theta, \varphi = 0$  or  $\pi$ ): aligning  $\mathbf{E}^{\text{dc}}$  and  $\nabla T^\omega$  along  $\pm x$  results in  $|\xi_N| = \xi_{yxxx}^{\text{BCP}}$ ,

showing that the electric-field-induced NANE originates solely from BCP; 2) Perpendicular alignment ( $\theta, \varphi = \pi/2, 3\pi/2$ ): aligning fields  $\mathbf{E}^{\text{dc}}$  and  $\nabla T^\omega$  to  $\pm y$  yields  $|\xi_N| = \xi_{xyyy}^{\text{BCP}}$ , indicating the BCP contribution dominates, whereas the contribution from the anomalous-velocity-modified NDF vanishes. Therefore, the geometric alignment of  $\mathbf{E}^{\text{dc}}$  and  $\nabla T^\omega$  eliminates the anomalous-velocity-modified-NDF contribution, confirming BCP as the sole origin of NANE in both cases.

#### IV. THE ELECTRIC-FIELD-INDUCED NONLINEAR ANOMALOUS NERNST EFFECT IN MONOLAYER GRAPHENE

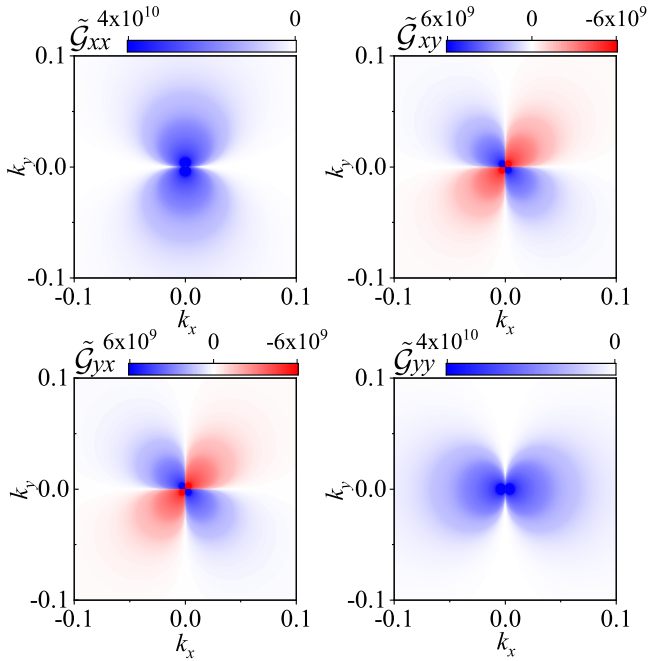


FIG. 2. Schematic of the Berry connection polarization elements  $\tilde{\mathcal{G}}_{xx}$  [(a)],  $\tilde{\mathcal{G}}_{xy}$  [(b)],  $\tilde{\mathcal{G}}_{yx}$  [(c)] and  $\tilde{\mathcal{G}}_{yy}$  [(d)] of the conduction band for the  $K$  valley of monolayer graphene. Momenta are measured in units of the inverse of the lattice constant  $\alpha$  and  $\tilde{\mathcal{G}}_{ab}$  is measured in units of  $e\alpha^2/t_0$

The point group symmetry  $C_{6v}$  of monolayer graphene includes a threefold rotation  $C_3$ , a twofold rotation  $C_2$  (an effective  $\mathcal{P}$  symmetry in 2D), and the mirror symmetry  $M_x$ . The presence of  $C_3$  and  $C_2$  symmetries suppresses the inherent NANE originating from  $\mathbf{A}^T$ . Additionally,  $\mathcal{T}$  symmetry forces both linear anomalous Nernst effect and intrinsic NANE vanish in monolayer graphene. Previously<sup>23</sup>, we proposed strain and substrate engineering to break these symmetries and induce NANE in the strained monolayer graphene. As shown in Table I, however, the electric-field-induced NANE are actually permitted under  $C_{6v}$  symmetry. Consequently, the NANE can emerge in the pristine monolayer graphene via electric field control, eliminating the need for additional

materials engineering.

The low-energy Hamiltonian of the monolayer graphene is<sup>38,39</sup>

$$\hat{H}_{\tau_v}(\mathbf{k}) = \tau_v v_F \hbar k_x \sigma_x + v_F \hbar k_y \sigma_y, \quad (15)$$

where  $x$  axis is selected as the zigzag direction,  $\tau_v = \pm 1$  is the valley index, the Fermi velocity  $v_F = \sqrt{3}\alpha t_0/2$  is determined by the lattice constant  $\alpha = 0.246 \text{ nm}$  and the nearest-neighbor hopping  $t_0 \approx 2.8 \text{ eV}$ , and  $\sigma$  represents the Pauli matrices for the two basis functions of energy band. This effective Hamiltonian  $\hat{H}_{\tau_v}(\mathbf{k})$  acts in the space of two-component wave functions  $\Phi = (\phi_A, \phi_B)$  with  $\phi_{\beta(A,B)}$  representing the electron amplitude on sublattices  $\beta$ . In this space, we have the group representation as  $\hat{\mathcal{T}} = \sigma_0 \mathcal{K}$ ,  $\hat{C}_2 = \sigma_x$ ,  $\hat{M}_x = \sigma_0$ ,  $\hat{M}_y = \sigma_x$ ,  $\hat{C}_3 = e^{\frac{2i\pi}{3}\tau_z\sigma_z}$ , and  $\hat{C}_3^2 = e^{-\frac{i2\pi}{3}\tau_z\sigma_z}$ . One can easily confirm  $\mathcal{T}$  and  $\mathcal{R} = [C_2, C_3, C_3^2, M_x]$  symmetries are present since  $\hat{H}_{\mathbf{K}'}(-\mathbf{k}) = \hat{\mathcal{T}}\hat{H}_{\mathbf{K}}(\mathbf{k})\hat{\mathcal{T}}^{-1}$  and  $\hat{H}_{\mathbf{R}\mathbf{K}}(\mathbf{R}\mathbf{k}) = \hat{\mathcal{R}}\hat{H}_{\mathbf{K}}(\mathbf{k})\hat{\mathcal{R}}^{-1}$  are satisfied, whereas the  $M_y$  symmetries is absent due to  $\hat{H}_{\mathbf{K}}(k_x, k_y) \neq \hat{M}_y^{-1}\hat{H}_{\mathbf{K}'}(k_x, -k_y)\hat{M}_y$ .

For simplicity, we only focus on  $n$ -doped systems. The corresponding energy dispersion  $\varepsilon_{\tau_v}(\mathbf{k})$  and BCP elements  $\tilde{\mathcal{G}}_{\tau_v,ab}(\mathbf{k})$  [Eq. (3)] for the conduction band of the monolayer graphene are found to be, respectively

$$\varepsilon_{\tau_v}(\mathbf{k}) = \hbar v_F k \quad (16)$$

$$\tilde{\mathcal{G}}_{\tau_v,ab}(\mathbf{k}) = \tilde{\mathcal{G}}_{ab}(\mathbf{k}) = \frac{e}{4\hbar v_F k^5} \begin{bmatrix} k_y^2 & -k_x k_y \\ -k_x k_y & k_x^2 \end{bmatrix},$$

showing that the both  $\varepsilon_{\tau_v}(\mathbf{k})$  and  $\tilde{\mathcal{G}}_{\tau_v,ab}(\mathbf{k})$  are independent of the valley index  $\tau_v$ . Consequently, the  $\xi_{abcd}^{\text{BCP}}$  [Eqs. (8) and (9)] at two valleys can have the same sign and contributes additively to NANE. The BCP elements [ $\tilde{\mathcal{G}}_{xx}$ ,  $\tilde{\mathcal{G}}_{xy}$ ,  $\tilde{\mathcal{G}}_{yx}$  and  $\tilde{\mathcal{G}}_{yy}$ ] for the monolayer graphene reaches their maximum around the Dirac cone [Fig. 2].

The  $C_{6v}$  symmetry of monolayer graphene guarantees that the angle-dependent scalar coefficient of electric-field-induced NANC  $\xi_N(\theta, \varphi)$  [Eq. (14)] only depends on the relative orientation of the applied  $\mathbf{E}^{\text{dc}}$  to the temperature gradient [Fig. 1]. Besides, the presence of both  $\mathcal{T}$  and  $\mathcal{P}$  symmetries forces  $\xi_{abcd}^{\text{NDF-}\mathcal{AV}} = 0$  (see details in Sec. III). Hence, the  $\xi_N(\theta, \varphi)$  in the monolayer graphene is reduced to be

$$\xi_N(\theta, \varphi) = \xi_{yxyy}^{\text{BCP}} \sin(\varphi - \theta), \quad (17)$$

showing that the NANE comes exclusively from the contribution from BCP [ $\xi_{yxyy}^{\text{BCP}}$ ] and exhibits a sine function dependence on the relative angle  $[\varphi - \theta]$  between the temperature gradient and  $\mathbf{E}^{\text{dc}}$  [Fig. 3(a)]. When applying  $\mathbf{E}^{\text{dc}}$  vertical to the temperature gradient (i.e.,  $\varphi - \theta = \pi/2, 3\pi/2$ ), the quantity  $|\xi_N(\theta, \varphi)|$  will reach its maximum, resulting in an extreme value of NANE in monolayer graphene. Conversely, when  $\mathbf{E}^{\text{dc}}$  is parallel or antiparallel to  $\nabla T^\omega$ ,  $\xi_N(\theta, \varphi) = 0$ , and the NANE disappears. A typical scale  $\xi_0 = 2\tau e^2 k_B^2 \alpha^2 / [(1 + i\omega\tau)\hbar^2 t_0]$  (where the factor 2 accounts for the spin degeneracy)

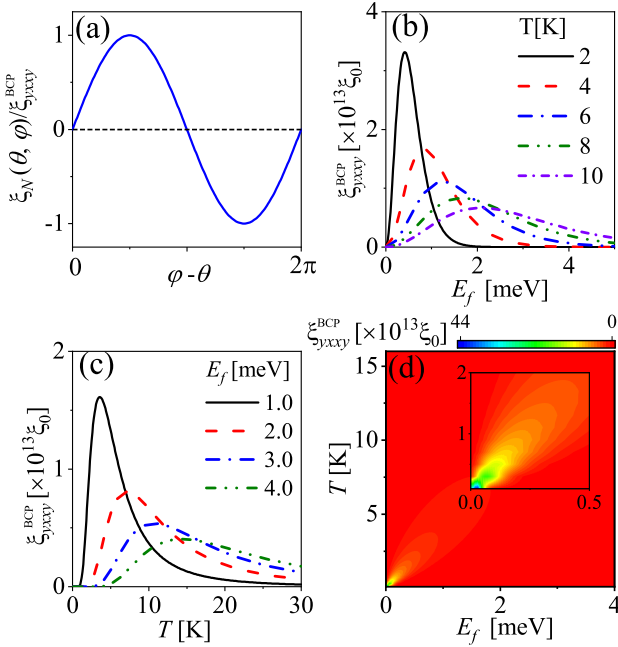


FIG. 3. (a) The dependence of  $\xi_N(\theta, \varphi)$  on the relative orientation (i.e.,  $\varphi - \theta$ ) of dc electric field  $\mathbf{E}^{dc}$  with respective to temperature gradient. (b)  $\xi_{yxy}^{BCP}$  versus the Fermi energy  $E_f$  for different temperature  $T$ . (c)  $\xi_{yxy}^{BCP}$  vs  $T$  for different  $E_f$ . (d)  $\xi_{yxy}^{BCP}$  as a function of  $E_f$  and  $T$ . The relative angle  $\varphi - \theta = \pi/2$  is fixed in (b)-(d). The typical scale  $\xi_0$  is defined as  $\xi_0 = 2\tau e^2 k_B \alpha^2 / [(1 + i\omega\tau) \hbar^2 t_0]$ .

is introduced to characterize the electric-field-induced NANE  $\xi_{yxy}^{BCP}$ .

Fig. 3(b) illustrates the dependence of coefficient  $\xi_{yxy}^{BCP}$  on the Fermi energy  $E_f$  for different temperature  $T$ . A peak feature of  $\xi_{yxy}^{BCP}$  is observed near the Dirac cone within 3 meV energy range. The emergence of this peak can be qualitatively attributed to the interplay between the rapid reduction of BCP and the linearly increasing density of states as the Fermi level moves away the Dirac point (i.e. as  $|E_f|$  increases). As  $T$  decreases, the value of the peak increases and its position shifts towards lower energy levels [Figs. 3(c) and 3(d)]. The largest values of  $\xi_{yxy}^{BCP}$  are observed at low temperatures and low Fermi energy levels (i.e., low  $n$  doping) [Fig. 3(d)].

When applying  $\mathbf{E}^{dc}$  vertical to  $\nabla T^\omega$  (i.e.,  $\varphi - \theta = \pi/2, 3\pi/2$ ), the second-harmonic nonlinear Nernst current in monolayer graphene is found to be  $j_N^{nl,2\omega} = \xi_{yxy}^{BCP} (\partial T) E$ , which corresponds to a second-harmonic Nernst voltage  $V_N^{2\omega} = W j_N^{nl,2\omega} / \sigma$  (see the details in Appendix D) in the open-circuit case with  $W$  being the width of the sample. The conductivity  $\sigma = n_c \mu e$  can be estimated as  $\tau E_f e^2 / \hbar^2 \pi$ , since the mobility  $\mu$  is expressed as  $\tau e/m$ , and meanwhile, for the monolayer graphene, we have the effective mass  $m = \hbar \sqrt{\pi n_c} / v_F$  and the carrier density  $n_c = E_f^2 / (v_F^2 \hbar^2 \pi)$ .<sup>39</sup> To numerically estimate the signal of the second-harmonic voltage drop origi-

nated from the electric-field-induced NANE in monolayer graphene, we take  $\xi_{yxy}^{BCP} = 3.14 \times 10^{13} \xi_0$  for  $T = 2$  K and  $E_f = 0.5$  meV. In the experiment, the amplitude of  $\nabla T^\omega$  can already reach 5 mK $\mu\text{m}^{-1}$ .<sup>25</sup> Therefore, in the low frequency limit  $\omega\tau \ll 1$ , the amplitude of the second-harmonic voltage ( $\text{Re}\{V^{2\omega}\}$ ) can reach 15.84 mV when  $W = 10 \mu\text{m}$  and  $E^{dc} = 1 \text{ V}/\mu\text{m}$ , which is in the same order of magnitude as the previously reported  $\Lambda^T$ -induced inherent NANE<sup>21–23</sup>.

## V. CONCLUSION

In summary, we have investigated the nonlinear Nernst effect as a second-order response to a alternating temperature gradient  $\nabla T^\omega$  under the control of the dc electric field  $\mathbf{E}^{dc}$ . It's found that a nonzero electric-field-induced NANE, linearly dependent on the relaxation time, can emerges owing to electric-field-corrected BC or the anomalous-velocity-modified NDF in  $\mathcal{T}$ -symmetric 2D materials with high crystal symmetries, where the intrinsic and  $\Lambda^T$ -induced inherent NANE is prohibited. Specially, we identify that when  $\mathbf{E}^{dc} \perp \nabla T^\omega$ , the electric-field-induced NANE is permissible across all the crystallographic symmetries applicable to 2D systems. The electric-field-induced NANE shows strong angular dependence on the orientation of  $\mathbf{E}^{dc}$  with respect to  $\nabla T^\omega$ , offering a route to control its signal. The behaviors of the NANE in the monolayer graphene have been investigated. Due to the simultaneous presence of  $\mathcal{T}$  and  $\mathcal{P}$  symmetry, both the inherent NANE from  $\Lambda^T$  and the electric-field-induced NANE originating from anomalous-velocity-modified-NDF contribution vanish, resulting in the electric-field-induced NANE from BCP determining the second-harmonic Nernst voltage in pristine monolayer graphene. Additionally, This electric-field-induced Nernst voltage in pristine monolayer graphene is in the same order of magnitude as the previously reported inherent NANE<sup>21–23</sup>.

## VI. ACKNOWLEDGEMENTS

This work is supported by the National Natural Science Foundation of China (Grant No. 12574073), and the National Science Foundation of Hunan, China (Grant No. 2023JJ30118)

## Appendix A: The distribution function $f(\mathbf{k})$ in the presence of temperature gradient and electric field

Within the relaxation time approximation, the Boltzmann equation for the electron distribution  $f(\mathbf{r}, \mathbf{k}, t)$ , which is a function of position  $\mathbf{r}$ , momentum  $\mathbf{k}$ , and time

$t$  is

$$\{\partial_t + \dot{\mathbf{r}} \cdot \nabla_{\mathbf{r}} + \dot{\mathbf{k}} \cdot \nabla_{\mathbf{k}}\}f(\mathbf{r}, \mathbf{k}, t) \approx -\frac{f(\mathbf{r}, \mathbf{k}, t) - f_0(\mathbf{k})}{\tau}, \quad (\text{A1})$$

where  $f_0 = 1/[\exp[(\varepsilon_{\mathbf{k}} - E_f)/k_B T] + 1]$  indicates the equilibrium Fermi distribution in absence of the external field, and  $\tau$  is the relaxation time. In absence of magnetic field, the semiclassical equation of the motion is

$$\begin{aligned} \dot{\mathbf{r}} &= \frac{1}{\hbar} \frac{\partial \varepsilon_{\mathbf{k}}}{\partial \mathbf{k}} - \dot{\mathbf{k}} \times \tilde{\boldsymbol{\Omega}}(\mathbf{k}), \\ \dot{\mathbf{k}} &= -\frac{e}{\hbar} \mathbf{E}, \end{aligned} \quad (\text{A2})$$

where  $\tilde{\boldsymbol{\Omega}}(\mathbf{k}) = \boldsymbol{\Omega}(\mathbf{k}) + \boldsymbol{\Omega}^E(\mathbf{k})$  represents the corrected BC by electric field with  $\boldsymbol{\Omega}(\mathbf{k})$  and  $\boldsymbol{\Omega}^E(\mathbf{k}) \propto \mathbf{E}$  representing the inherent and electric-field-corrected BC, respectively. We consider an *alternating* temperature gradient  $\nabla T^\omega(t) = \text{Re}\{\tilde{\nabla}T e^{i\omega t}\}$  (where complex amplitude vector  $\tilde{\nabla}T$  is independent of the time), which can be experimentally realized by passing an alternating current  $I_h^\omega = I_0 \sin(\omega' t + \phi_0)$  ( $\omega' = \omega/2$ ,  $\phi_0$  indicates the initial phase) through a microheater electrode<sup>25</sup>. The corresponding complex amplitude vector is given by  $\tilde{\nabla}T = \hat{n} Q I_0^2 e^{i\pi + i\phi_0}/2$  with  $Q$  representing proportionality coef-

ficient and  $\hat{n}$  indicating the unit vector along the temperature gradient. The local distribution function  $f(\mathbf{r}, \mathbf{k}, t)$  fixed itself by the temperature at  $\mathbf{r}$ , can be then determined as

$$\nabla_{\mathbf{r}} f = \nabla_{\mathbf{r}} T(t) \frac{\partial f}{\partial T} = \text{Re}\{\tilde{\nabla}T e^{i\omega t}\} \frac{\partial f}{\partial T}. \quad (\text{A3})$$

Combining Eqs. (A1) (A2) and Eq. (A3), we have

$$\begin{aligned} \frac{f_0 - f}{\tau} &= \left[ \left( \frac{1}{\hbar} \frac{\partial \varepsilon_{\mathbf{k}}}{\partial \mathbf{k}} + \frac{e}{\hbar} (\mathbf{E} \times \tilde{\boldsymbol{\Omega}}) \right) \cdot \text{Re}\{\tilde{\nabla}T e^{i\omega t}\} \frac{\partial}{\partial T} \right. \\ &\quad \left. - \frac{e}{\hbar} \mathbf{E} \cdot \nabla_{\mathbf{k}} + \partial_t \right] f. \end{aligned} \quad (\text{A4})$$

$f$  can be expressed as a perturbation expansion:

$$f = f_0 + \sum_{n,m} \delta f^{(n,m)}, \quad (\text{A5})$$

where  $\delta f^{(n,m)}$  represents the component of nonequilibrium distribution corresponding to the  $n$ -th order in electric field  $E$  and  $m$ -th order in the amplitude of temperature gradient  $\text{Re}\{\tilde{\nabla}T\}$ . Taking Eq. (A5) into Eq. (A4) and comparing the expansion order, one can obtain a recursive equation for  $\delta f^{(n,m)}$  as

$$\begin{aligned} -\frac{\delta f^{(n,m)}}{\tau} &= \partial_t f^{(n,m)} - \frac{e}{\hbar} \mathbf{E} \cdot \nabla_{\mathbf{k}} \delta f^{(n-1,m)} + \sum_l \left( \frac{1}{\hbar} \frac{\partial \varepsilon_{\mathbf{k}}}{\partial \mathbf{k}} \right)^{(l)} \cdot \frac{1}{2} \left[ \tilde{\nabla}T e^{i\omega t} + (\tilde{\nabla}T)^* e^{-i\omega t} \right] \frac{\partial \delta f^{(n-l,m-1)}}{\partial T} \\ &\quad + \sum_l \frac{e}{\hbar} (\mathbf{E} \times \tilde{\boldsymbol{\Omega}})^{(l)} \cdot \frac{1}{2} \left[ \tilde{\nabla}T e^{i\omega t} + (\tilde{\nabla}T)^* e^{-i\omega t} \right] \frac{\partial \delta f^{(n-l,m-1)}}{\partial T}. \end{aligned} \quad (\text{A6})$$

We are interested in computing the response to second order in the temperature gradient and the first order in the electric field, hence, we will only calculate the distribution up to the second order in the temperature gradient and the first order in the electric field, namely  $f \approx \text{Re}\{f_0 + \delta f^{(1,0)} + \delta f^{(0,1)} + \delta f^{(1,1)} + \delta f^{(0,2)}\}$ . By iteration, these leading orders [ $\delta f^{(1,0)}$ ,  $\delta f^{(0,1)}$ ,  $\delta f^{(1,1)}$  and  $\delta f^{(0,2)}$ ] are determined as, respectively

$$\begin{aligned} \delta f^{(1,0)} &= \frac{e\tau}{\hbar} \mathbf{E} \cdot \nabla_{\mathbf{k}} f_0, & \delta f^{(0,1)} &= \delta f_\omega^{(0,1)} e^{i\omega t}, \\ \delta f^{(1,1)} &= \delta f_\omega^{(1,1)} e^{i\omega t}, & \delta f^{(0,2)} &= \delta f_0^{(0,2)} + \delta f_{2\omega}^{(0,2)} e^{2i\omega t}, \end{aligned} \quad (\text{A7})$$

with

$$\begin{aligned} \delta f_\omega^{(0,1)} &= -\frac{\tau \mathbf{v} \cdot \tilde{\nabla}T}{(1 + i\omega\tau)} \frac{\partial f_0}{\partial T}, \\ \delta f_\omega^{(1,1)} &= \frac{\tau}{(1 + i\omega\tau)} \left[ \frac{e}{\hbar} \mathbf{E} \cdot \nabla_{\mathbf{k}} \delta f_\omega^{(0,1)} - \mathbf{v} \cdot \tilde{\nabla}T \frac{\partial \delta f^{(1,0)}}{\partial T} \right. \\ &\quad \left. - \left( \frac{e}{\hbar} \mathbf{E} \times \tilde{\boldsymbol{\Omega}} \right) \cdot \tilde{\nabla}T \frac{\partial f_0}{\partial T} \right], \\ \delta f_0^{(0,2)} &= -\frac{\tau \mathbf{v} \cdot (\tilde{\nabla}T)^*}{2} \frac{\partial \delta f_\omega^{(0,1)}}{\partial T}, \\ \delta f_{2\omega}^{(0,2)} &= -\frac{\tau \mathbf{v} \cdot \tilde{\nabla}T}{2(1 + 2i\omega\tau)} \frac{\partial \delta f_\omega^{(0,1)}}{\partial T}, \end{aligned} \quad (\text{A8})$$

where the equality  $\partial \varepsilon_{\mathbf{k}} / \partial \mathbf{k} = \hbar \mathbf{v}$  has been used for simplicity. One might notice the following relation

$$\frac{\partial f_0}{\partial T} = -\frac{(\varepsilon_{\mathbf{k}} - E_f)}{T} \frac{\partial f_0}{\partial \varepsilon_{\mathbf{k}}}. \quad (\text{A9})$$

Combining Eq. (A9) with equality  $\partial \varepsilon_{\mathbf{k}} / \partial \mathbf{k} = \hbar \mathbf{v}$ , we can

further transform  $\partial f_0 / \partial T$  into  $\partial f_0 / \partial \mathbf{k}$  through the differential treatment, namely

$$\frac{\partial f_0}{\partial \mathbf{k}} = \frac{\partial f_0}{\partial \varepsilon_{\mathbf{k}}} \frac{\partial \varepsilon_{\mathbf{k}}}{\partial \mathbf{k}} = -\frac{\hbar v T}{(\varepsilon_{\mathbf{k}} - E_f)} \frac{\partial f_0}{\partial T}, \quad (\text{A10})$$

giving the following identities

$$\begin{aligned} \frac{\partial f_0}{\partial T} v_a &= -\frac{\varepsilon_{\mathbf{k}} - E_f}{\hbar T} \frac{\partial f_0}{\partial k_a}, \\ \frac{\partial^2 f_0}{\partial T^2} v_a v_b &= 2 \frac{\varepsilon_{\mathbf{k}} - E_f}{\hbar T^2} \frac{\partial f_0}{\partial k_a} v_b + \left( \frac{\varepsilon_{\mathbf{k}} - E_f}{\hbar T} \right)^2 \frac{\partial^2 f_0}{\partial k_a \partial k_b}. \end{aligned} \quad (\text{A11})$$

Using these two identities, the coefficients  $[\delta f_{\omega}^{(0,1)}, \delta f_{\omega}^{(1,1)}, \delta f_0^{(0,2)} \text{ and } \delta f_{2\omega}^{(0,2)}]$  in Eq. (A8) can be further simplified as

$$\begin{aligned} \delta f_{\omega}^{(0,1)} &= \frac{\tau (\varepsilon_{\mathbf{k}} - E_f)}{(1 + i\omega\tau) T \hbar} \frac{\partial f_0}{\partial k_a} \partial_a \tilde{T}, \\ \delta f_{\omega}^{(1,1)} &= \left\{ \frac{e\tau^2 (2 + i\omega\tau)}{(1 + i\omega\tau)^2 \hbar^2 T} \left[ (\varepsilon_{\mathbf{k}} - E_f) \frac{\partial^2 f_0}{\partial k_a \partial k_b} + \hbar v_b \frac{\partial f_0}{\partial k_a} \right] \right. \\ &\quad \left. + \epsilon_{abc} \frac{e\tau}{(1 + i\omega\tau) \hbar} \Omega_c \frac{(\varepsilon_{\mathbf{k}} - E_f)}{T} \frac{\partial f_0}{\partial \varepsilon_{\mathbf{k}}} \right\} \partial_a T E_b, \\ \delta f_0^{(0,2)} &= \frac{\tau^2}{2(1 + i\omega\tau)} \left[ \frac{2(\varepsilon_{\mathbf{k}} - E_f)}{\hbar T^2} \frac{\partial f_0}{\partial k_a} v_b + \frac{(\varepsilon_{\mathbf{k}} - E_f)^2}{\hbar^2 T^2} \right. \\ &\quad \left. \times \frac{\partial^2 f_0}{\partial k_a \partial k_b} \right] (\partial_a \tilde{T})^* \partial_b \tilde{T}, \\ \delta f_{2\omega}^{(0,2)} &= \frac{\tau^2}{2(1 + i\omega\tau)(1 + 2i\omega\tau)} \left[ \frac{2(\varepsilon_{\mathbf{k}} - E_f)}{\hbar T^2} \frac{\partial f_0}{\partial k_a} v_b \right. \\ &\quad \left. + \frac{(\varepsilon_{\mathbf{k}} - E_f)^2}{\hbar^2 T^2} \frac{\partial^2 f_0}{\partial k_a \partial k_b} \right] \partial_a \tilde{T} \partial_b \tilde{T}. \end{aligned} \quad (\text{A12})$$

## Appendix B: The electric-field-induced nonlinear anomalous Nernst effect in $\mathcal{T}$ -symmetric systems

Accompanying Eq. (4) with Eqs. (A7) and (A12), the thermally driven nonlinear current density  $j_a^{\text{nl}}$  in  $a$  direction, as a second-order response to the alternating temperature gradient  $\nabla T^{\omega}$  in the presence of a dc electric field  $\mathbf{E}^{\text{dc}}$ , can be expressed as

$$j_a^{\text{nl}} = \text{Re}\{j_a^{\text{nl},0} + j_a^{\text{nl},2\omega} e^{2i\omega t}\}, \quad (\text{B1})$$

where the rectified current  $j_a^{\text{nl},0}$  and the second-harmonic term  $j_a^{\text{nl},2\omega}$  are determined as, respectively,

$$\begin{aligned} j_a^{\text{nl},0} &= -e \int [d\mathbf{k}] \dot{r}_a \delta f_0^{(0,2)} - \epsilon_{abl} \frac{e}{2\hbar T} \int [d\mathbf{k}] \tilde{\Omega}_l(\mathbf{k}) \\ &\quad \times (\varepsilon_{\mathbf{k}} - E_f) \left[ \delta f_{\omega}^{(0,1)} + \delta f_{\omega}^{(1,1)} \right] (\partial_b \tilde{T})^*, \\ j_a^{\text{nl},2\omega} &= -e \int [d\mathbf{k}] \dot{r}_a \delta f_{2\omega}^{(0,2)} - \epsilon_{abl} \frac{e}{2\hbar T} \int [d\mathbf{k}] \tilde{\Omega}_l(\mathbf{k}) \\ &\quad \times (\varepsilon_{\mathbf{k}} - E_f) \left[ \delta f_{\omega}^{(0,1)} + \delta f_{\omega}^{(1,1)} \right] \partial_b \tilde{T}, \end{aligned} \quad (\text{B2})$$

where  $\epsilon_{abl}$  is the Levi-Civita symbol, the indices  $(a, b, l)$  represent the cartesian components and the repeated indices are summed over. According to Eq. (A12), one can easily observe that both  $\text{Re}\{\delta f_{\omega}^{(0,1)}\}$  (linear to  $\tau$ ) and  $\text{Re}\{\delta f_{\omega}^{(1,1)}\}$  (one component  $\propto \tau$  while others  $\propto \tau^2$ ) are linearly dependent of the amplitude of temperature gradient  $\text{Re}\{\partial_d \tilde{T}\}$ , while  $\text{Re}\{\delta f_{2\omega}^{(0,2)}\}$  and  $\text{Re}\{\delta f_0^{(0,2)}\}$  (quadratic to  $\tau$ ) quadratically depends on  $\text{Re}\{\partial_d \tilde{T}\}$ . Under  $\mathcal{T}$  symmetry, the current  $j_a^{\text{nl}}$  and  $\tau$  change sign but temperature gradient keeps unchanged, restricting the  $\tau$ -even dependent component of the current vanishing<sup>41,42</sup>. Therefore, only the terms related to  $\delta f_{\omega}^{(0,1)}$  and  $\tau$ -odd component of  $\delta f_{\omega}^{(1,1)}$  [Eq. (A12)] in Eq. (B2) contribute to thermally driven nonlinear current  $j_a^{\text{nl}}$  in  $\mathcal{T}$ -symmetric systems, which is we focus on this work. One can also confirm that these nonzero nonlinear current are vertical to temperature gradient, namely the Nernst current, since the first term ( $\propto \delta f_0^{(0,2)}$ ) in Eq. (B2) has no contribution in  $\mathcal{T}$ -symmetric systems while the nonlinear current from the second terms are actually perpendicular to the temperature gradient. Consequently, after a tedious derivation, the nonzero components  $j_a^{\text{nl},0}$  and  $j_a^{\text{nl},2\omega}$  of the nonlinear Nernst current, to first-order approximation of the electric field, in  $\mathcal{T}$ -symmetric systems are found to be

$$\begin{aligned} j_a^{\text{nl},0} &= (\chi_{abc} + \xi_{abcd} E_d) (\partial_b \tilde{T})^* \partial_c \tilde{T}, \\ j_a^{\text{nl},2\omega} &= (\chi_{abc} + \xi_{abcd} E_d) \partial_b \tilde{T} \partial_c \tilde{T} \end{aligned} \quad (\text{B3})$$

with

$$\begin{aligned} \chi_{abc} &= \frac{-\tau e \epsilon_{abl}}{2(1 + i\omega\tau) \hbar^2} \int [d\mathbf{k}] \Omega_l(\mathbf{k}) \frac{(\varepsilon_{\mathbf{k}} - E_f)^2}{T^2} \frac{\partial f_0}{\partial k_c}, \\ \xi_{abcd} &= \frac{-\tau e \epsilon_{abl}}{2(1 + i\omega\tau) \hbar^2} \left[ \epsilon_{lgv} \int [d\mathbf{k}] \frac{\partial \tilde{\mathcal{G}}_{vd}(\mathbf{k})}{\partial k_g} \frac{(\varepsilon_{\mathbf{k}} - E_f)^2}{T^2} \frac{\partial f_0}{\partial k_c} \right. \\ &\quad \left. + e \epsilon_{cdu} \int [d\mathbf{k}] \Omega_l(\mathbf{k}) \Omega_u(\mathbf{k}) \frac{(\varepsilon_{\mathbf{k}} - E_f)^2}{T^2} \frac{\partial f_0}{\partial \varepsilon_{\mathbf{k}}} \right]. \end{aligned} \quad (\text{B4})$$

Obviously, both nonzero coefficients  $\chi_{abc}$  and  $\xi_{abcd}$  in  $\mathcal{T}$ -symmetric systems have been restricted to be odd functions of  $\tau$ , hinting  $\mathcal{T}$ -odd property. Additionally, one can also intuitively confirm this  $\mathcal{T}$ -odd character based on Eq. (B3). Under  $\mathcal{T}$  symmetry, only  $j_a^{\text{nl}}$  changes sign, while both temperature gradient and electric field keep unchanged, enforcing  $\chi_{abc}$  and  $\xi_{abcd}$   $\mathcal{T}$ -odd.

Equation (B4) shows the coefficient  $\chi_{abc}$  is proportional to a pseudotensorial quantity  $\Lambda_{lc}^T$ , defined as

$$\Lambda_{lc}^T = - \int [d\mathbf{k}] \Omega_l(\mathbf{k}) \frac{(\varepsilon_{\mathbf{k}} - E_f)^2}{T^2} \frac{\partial f_0}{\partial k_c}, \quad (\text{B5})$$

which was firstly defined and analyzed by Yu *et al.*<sup>21</sup>, and play as the quantum origin to generate the inherent NANE. This novel pseudotensorial quantity  $\Lambda_{lc}^T$  stems from the BC near the Fermi surface, and features an extra factor  $(\varepsilon_{\mathbf{k}} - E_f)^2/T^2$  in integral comparing the BCD<sup>4</sup>,  $D_{lc} = - \int [d\mathbf{k}] \Omega_l(\mathbf{k}) \partial_{k_c} f_0$ . The first term of the coefficient  $\xi_{abcd}$  in Eq. (B4) comes from the BCP rooting in the electric-field-induced BC  $\Omega^E(\mathbf{k})$ , and the second term actually comes from the anomalous velocity  $(\mathbf{E} \times \mathbf{\Omega})$  corrected NDF. The coefficients  $\xi_{abcd}$  thus can be decomposed into two parts as

$$\xi_{abcd} = \frac{\tau e \epsilon_{abl}}{2(1 + i\omega\tau)\hbar^2} (\Upsilon_{lcd} + e \epsilon_{cd} \Gamma_{lu}) \quad (\text{B6})$$

with

$$\begin{aligned} \Upsilon_{lcd} &= -\epsilon_{lgv} \int [d\mathbf{k}] \frac{\partial \tilde{\mathcal{G}}_{vd}(\mathbf{k})}{\partial k_g} \frac{(\varepsilon_{\mathbf{k}} - E_f)^2}{T^2} \frac{\partial f_0}{\partial k_c}, \\ \Gamma_{lu} &= - \int [d\mathbf{k}] \Omega_l(\mathbf{k}) \Omega_u(\mathbf{k}) \frac{(\varepsilon_{\mathbf{k}} - E_f)^2}{T^2} \frac{\partial f_0}{\partial \varepsilon_{\mathbf{k}}}. \end{aligned} \quad (\text{B7})$$

In 2D crystals, the inherent and field-corrected BC transforms from a pseudovector to a pseudoscalar, and only the out-of-plane component [i.e.  $\Omega_{l=\mu=z}(\mathbf{k})$  and  $\Omega_{l=z}^E(\mathbf{k})$ ] can be nonzero, enforcing the indices  $[l, \mu]$  in Eqs. (B4)-(B7) fixed to be  $z$ . Consequently, the pseudotensorial quantity  $\Lambda_{cd}^T$  behaves as a pseudovector, while the third-order pseudotensorial quantity  $\Upsilon_{lcd}$  (pseudotensorial  $\Gamma_{lu}$ ) behave as a pseudotensorial (scalar) quantity contained

in the 2D plane, respectively:

$$\begin{aligned} \Lambda_c^T &= - \int [d\mathbf{k}] \Omega_z(\mathbf{k}) \frac{(\varepsilon_{\mathbf{k}} - E_f)^2}{T^2} \frac{\partial f_0}{\partial k_c}, \\ \Upsilon_{cd} &= \int [d\mathbf{k}] \left[ \frac{\partial \tilde{\mathcal{G}}_{xd}(\mathbf{k})}{\partial k_y} - \frac{\partial \tilde{\mathcal{G}}_{yd}(\mathbf{k})}{\partial k_x} \right] \frac{(\varepsilon_{\mathbf{k}} - E_f)^2}{T^2} \frac{\partial f_0}{\partial k_c}, \\ \Gamma &= - \int [d\mathbf{k}] \Omega_z^2(\mathbf{k}) \frac{(\varepsilon_{\mathbf{k}} - E_f)^2}{T^2} \frac{\partial f_0}{\partial \varepsilon_{\mathbf{k}}}. \end{aligned} \quad (\text{B8})$$

As a result, the rectified current  $\mathbf{j}^{\text{nl},0}$  and the second-harmonic term  $\mathbf{j}^{\text{nl},2\omega}$  for the 2D systems can be written in vector notation as, respectively,

$$\begin{aligned} \mathbf{j}^{\text{nl},0} &= \frac{e\tau}{2(1 + i\omega\tau)\hbar^2} (\hat{z} \times (\tilde{\nabla}T)^*) (\tilde{\nabla}T \cdot \mathbf{\Lambda}^T) \\ &+ \frac{e\tau}{2(1 + i\omega\tau)\hbar^2} (\hat{z} \times (\tilde{\nabla}T)^*) (\tilde{\nabla}T \cdot \overleftrightarrow{\Upsilon}) \cdot \mathbf{E} \\ &+ \frac{e^2\tau\Gamma}{(1 + i\omega\tau)\hbar^2} (\hat{z} \times (\tilde{\nabla}T)^*) (\hat{z} \times \tilde{\nabla}T) \cdot \mathbf{E}, \end{aligned} \quad (\text{B9})$$

and

$$\begin{aligned} \mathbf{j}^{\text{nl},2\omega} &= \frac{e\tau}{2(1 + i\omega\tau)\hbar^2} (\hat{z} \times \tilde{\nabla}T) (\tilde{\nabla}T \cdot \mathbf{\Lambda}^T) \\ &+ \frac{e\tau}{2(1 + i\omega\tau)\hbar^2} (\hat{z} \times \tilde{\nabla}T) (\tilde{\nabla}T \cdot \overleftrightarrow{\Upsilon}) \cdot \mathbf{E} \\ &+ \frac{e^2\tau\Gamma}{(1 + i\omega\tau)\hbar^2} (\hat{z} \times \tilde{\nabla}T) (\hat{z} \times \tilde{\nabla}T) \cdot \mathbf{E}. \end{aligned} \quad (\text{B10})$$

### Appendix C: Angular dependence of the electric-field-induced nonlinear anomalous Nernst coefficient

We consider the 2D case with  $\mathcal{T}$  symmetry and assume a principal crystal axis along  $x$ -direction. Then, the nonlinear second harmonic response along  $x$  and  $y$ -direction in this Cartesian coordinate can be written as

$$\begin{pmatrix} j_x^{\text{nl},2\omega} \\ j_y^{\text{nl},2\omega} \end{pmatrix} = \begin{pmatrix} 0 & 0 & 0 & 0 & -\xi_{yxxx} & -\xi_{yxxz} & \xi_{xyyx} & \xi_{xyyy} \\ \xi_{yxxx} & \xi_{yxxz} & -\xi_{xyyx} & -\xi_{xyyy} & 0 & 0 & 0 & 0 \end{pmatrix} \begin{pmatrix} \partial_x \tilde{T} \partial_x \tilde{T} E_x \\ \partial_x \tilde{T} \partial_x \tilde{T} E_y \\ \partial_x \tilde{T} \partial_y \tilde{T} E_x \\ \partial_x \tilde{T} \partial_y \tilde{T} E_y \\ \partial_y \tilde{T} \partial_x \tilde{T} E_x \\ \partial_y \tilde{T} \partial_x \tilde{T} E_y \\ \partial_y \tilde{T} \partial_y \tilde{T} E_x \\ \partial_y \tilde{T} \partial_y \tilde{T} E_y \end{pmatrix}. \quad (\text{C1})$$

To obtain Eq. (C1), the relations  $\xi_{abcd} = -\xi_{bacd}$  with  $a$  and  $b = \{x, y\}$  [see details in Sec. III] have been

used. When one transforms the principal axis coordinate into the coordinates defined by the measurement

setup [Fig. 1], in which  $\parallel$  is the direction of the temperature gradient (meaning  $\partial_{\parallel} T = 0$ ) and  $\perp$  represents the Nernst current direction perpendicularly to the temperature gradient, the nonlinear second harmonic current, temperature gradient and electric field transforms as, respectively

$$\begin{pmatrix} j_x^{\text{nl},2\omega} \\ j_y^{\text{nl},2\omega} \end{pmatrix} = \begin{pmatrix} \cos \theta & -\sin \theta \\ \sin \theta & \cos \theta \end{pmatrix} \begin{pmatrix} j_{\parallel}^{\text{nl},2\omega} \\ j_{\perp}^{\text{nl},2\omega} \end{pmatrix}, \quad (\text{C2})$$

$$\begin{pmatrix} \partial_x \tilde{T} \\ \partial_y \tilde{T} \end{pmatrix} = \begin{pmatrix} \cos \theta \\ \sin \theta \end{pmatrix} \partial \tilde{T}, \quad (\text{C3})$$

$$\begin{pmatrix} E_x \\ E_y \end{pmatrix} = \begin{pmatrix} \cos \theta & -\sin \theta \\ \sin \theta & \cos \theta \end{pmatrix} \begin{pmatrix} E_{\parallel} \\ E_{\perp} \end{pmatrix} = E \begin{pmatrix} \cos \theta & -\sin \theta \\ \sin \theta & \cos \theta \end{pmatrix} \begin{pmatrix} \cos(\varphi - \theta) \\ \sin(\varphi - \theta) \end{pmatrix}, \quad (\text{C4})$$

where the  $\theta$  ( $\varphi$ ) indicates the polar angle of the temperature gradient  $\nabla T$  (the dc electric field  $\mathbf{E}^{\text{dc}}$ ) measured from the  $x$  direction, and  $\tilde{\partial}T = \partial_{\parallel} T = [(\partial_x T)^2 + (\partial_y T)^2]^{1/2}$  indicates the amplitude of the temperature gradient for simplification. According to the transform relations of temperature gradient [Eq. (C3)] and electric field [Eq. (C4)], we can have

$$\begin{pmatrix} \partial_x \tilde{T} \partial_x \tilde{T} E_x \\ \partial_x \tilde{T} \partial_x \tilde{T} E_y \\ \partial_x \tilde{T} \partial_y \tilde{T} E_x \\ \partial_x \tilde{T} \partial_y \tilde{T} E_y \\ \partial_y \tilde{T} \partial_x \tilde{T} E_x \\ \partial_y \tilde{T} \partial_x \tilde{T} E_y \\ \partial_y \tilde{T} \partial_y \tilde{T} E_x \\ \partial_y \tilde{T} \partial_y \tilde{T} E_y \end{pmatrix} = \begin{pmatrix} \cos^2 \theta \cos \varphi \\ \cos^2 \theta \sin \varphi \\ \sin \theta \cos \theta \cos \varphi \\ \sin \theta \cos \theta \sin \varphi \\ \sin \theta \cos \theta \cos \varphi \\ \sin \theta \cos \theta \sin \varphi \\ \sin^2 \theta \cos \varphi \\ \sin^2 \theta \sin \varphi \end{pmatrix} \tilde{\partial}T \tilde{\partial}T E. \quad (\text{C5})$$

Combining the relations with Eqs. (C5) (C1) and (C2), one can obtain

$$\begin{aligned} j_{\parallel}^{\text{nl},2\omega} &= 0, \\ j_{\perp}^{\text{nl},2\omega} &= \xi_N(\theta, \varphi) \tilde{\partial}T \tilde{\partial}T E, \end{aligned} \quad (\text{C6})$$

with the angle-dependent scalar coefficient determined by

$$\begin{aligned} \xi_N(\theta, \varphi) &= (\xi_{yxxx} \cos \varphi + \xi_{yxx} \sin \varphi) \cos \theta \\ &\quad - (\xi_{xyyx} \cos \varphi + \xi_{xyyy} \sin \varphi) \sin \theta. \end{aligned} \quad (\text{C7})$$

#### Appendix D: The angular dependence of the nonlinear Nernst voltage

We have analyzed that angular dependence of the electric-field-induced NANC  $\xi_N(\theta, \varphi)$  in appendix C. However, what is measured in experiments is the nonlinear Hall voltage, which will be derived in this appendix based on Ohm's law. The detected Nernst second-harmonic voltage  $V_{\perp}^{2\omega}$  as a second-order response to alternating temperature gradient via NANE can be written as

$$V_{\perp}^{2\omega} = W E_{\perp}^{2\omega}, \quad (\text{D1})$$

where  $W$  indicates the width of sample vertical to the temperature gradient, and  $E_{\perp}^{2\omega}$  represents the induced electric field perpendicular to temperature gradient owing to the NANE, which can be determined through the generated second-harmonic currents  $j_{\parallel}^{\text{nl},2\omega}$  ( $j_{\perp}^{\text{nl},2\omega}$ ) parallel (perpendicular) to temperature gradient as follows. When transforming the coordinates defined by the measurement setup [Fig. 1] into the principal coordinate (having assumed a principal crystal direction along  $x$  axis), we have

$$\begin{pmatrix} j_{\parallel}^{\text{nl},2\omega} \\ j_{\perp}^{\text{nl},2\omega} \end{pmatrix} = \begin{pmatrix} \cos \theta & \sin \theta \\ -\sin \theta & \cos \theta \end{pmatrix} \begin{pmatrix} j_x^{\text{nl},2\omega} \\ j_y^{\text{nl},2\omega} \end{pmatrix}, \quad (\text{D2})$$

and

$$\begin{pmatrix} E_{\perp}^{2\omega} \\ E_{\parallel}^{2\omega} \end{pmatrix} = \begin{pmatrix} \cos \theta & \sin \theta \\ -\sin \theta & \cos \theta \end{pmatrix} \begin{pmatrix} E_x^{2\omega} \\ E_y^{2\omega} \end{pmatrix}, \quad (\text{D3})$$

In addition, according to Ohm's law, we have the relation between the second-harmonic current  $j_x^{\text{nl},2\omega}$  ( $j_y^{\text{nl},2\omega}$ ), parallel (perpendicular) to the principal axis (i.e.  $x$  axis) of the system, and the conductivity  $\sigma$  as  $j_x^{\text{nl},2\omega} = \sigma_{xx} E_x^{2\omega}$  ( $j_y^{\text{nl},2\omega} = \sigma_{yy} E_y^{2\omega}$ ). When combining these relation with Eqs. (D2) and (D3), yielding

$$\begin{aligned} E_{\perp}^{2\omega} &= j_{\perp}^{\text{nl},2\omega} \left( \frac{\sin^2 \theta}{\sigma_{xx}} + \frac{\cos^2 \theta}{\sigma_{yy}} \right), \\ E_{\parallel}^{2\omega} &= j_{\parallel}^{\text{nl},2\omega} \left( \frac{1}{\sigma_{yy}} - \frac{1}{\sigma_{xx}} \right) \sin \theta \cos \theta. \end{aligned} \quad (\text{D4})$$

Combining Eq.(D4) with Eq.(D1) and assuming  $\sigma_{xx} = \sigma_{yy}$ , the second-harmonic Nernst voltage  $V_{\perp}^{2\omega}$  can be expressed as

$$V_{\perp}^{2\omega} = \frac{W j_{\perp}^{\text{nl},2\omega}}{\sigma_{xx}}. \quad (\text{D5})$$

The  $j_{\perp}^{\text{nl},2\omega}$ , perpendicular to the temperature gradient, indicate the second-harmonic component of the nonlinear Nernst current and, therefore, has been written as  $j_N^{\text{nl},2\omega}$  in the main text.

\* yuxiaoqin@hnu.edu.cn

- <sup>1</sup> Z. Qiao, S. A. Yang, W. Feng, W.-K. Tse, J. Ding, Y. Yao, J. Wang, and Q. Niu, Quantum anomalous Hall effect in graphene from Rashba and exchange effects, *Phys. Rev. B* **82**, 161414(R) (2010).
- <sup>2</sup> G. Xu, H. Weng, Z. Wang, X. Dai, and Z. Fang, Chern semimetal and the quantized anomalous Hall effect in HgCr<sub>2</sub>Se<sub>4</sub>, *Phys. Rev. Lett.* **107**, 186806 (2011).
- <sup>3</sup> D. Xiao, Y. Yao, Z. Fang, and Q. Niu, Berry-phase effect in anomalous thermoelectric transport, *Phys. Rev. Lett.* **97**, 026603 (2006).
- <sup>4</sup> I. Sodemann and L. Fu, Quantum nonlinear Hall effect induced by Berry curvature dipole in time-reversal invariant materials, *Phys. Rev. Lett.* **115**, 216806 (2015).
- <sup>5</sup> T. Low, Y. Jiang, and F. Guinea, Topological currents in black phosphorus with broken inversion symmetry, *Phys. Rev. B* **92**, 235447 (2015).
- <sup>6</sup> Z. Z. Du, C. M. Wang, H.-Z. Lu, and X. C. Xie, Band signatures for strong nonlinear Hall effect in bilayer WTe<sub>2</sub>, *Phys. Rev. Lett.* **121**, 266601 (2018).
- <sup>7</sup> Z. Du, C. Wang, S. Li, H.-Z. Lu, and X. Xie, Disorder-induced nonlinear Hall effect with time-reversal symmetry, *Nat. Commun.* **10**, 3047 (2019).
- <sup>8</sup> R. Battilomo, N. Scopigno, and C. Ortix, Berry curvature dipole in strained graphene: A Fermi surface warping effect, *Phys. Rev. Lett.* **123**, 196403 (2019).
- <sup>9</sup> J. I. Facio, D. Efremov, K. Koepernik, J.-S. You, I. Sodemann, and J. van den Brink, Strongly enhanced Berry dipole at topological phase transitions in BiTeI, *Phys. Rev. Lett.* **121**, 246403 (2018).
- <sup>10</sup> Z. Du, C. Wang, H.-P. Sun, H.-Z. Lu, and X. Xie, Quantum theory of the nonlinear Hall effect, *Nat. Commun.* **12**, 5038 (2021).
- <sup>11</sup> A. Bandyopadhyay, N. B. Joseph, and A. Narayan, Nonlinear Hall effects: Mechanisms and materials, *Mater. Today Electron.* **8** 100101 (2024).
- <sup>12</sup> W. Miao, W.-L. Zhen, C. Tan, J. Wang, Y. Nie, H. Wang, L. Wang, Q. Niu and M.-L. Tian, Nonreciprocal antisymmetric magnetoresistance and unconventional Hall effect in a two-dimensional ferromagnet, *ACS Nano* **17**, 25449 (2023).
- <sup>13</sup> D. Kaplan, T. Holder, and B. Yan, Unification of nonlinear anomalous Hall effect and nonreciprocal magnetoresistance in metals by the quantum geometry, *Phys. Rev. Lett.* **132**, 026301 (2024).
- <sup>14</sup> V. A. Zyuzin, In-plane hall effect in two-dimensional helical electron systems, *Phys. Rev. B* **102**, 241105(R) (2020).
- <sup>15</sup> H. Wang, Y.-X. Huang, H. Liu, X. Feng, J. Zhu, W. Wu, C. Xiao, and S. A. Yang, Orbital origin of the intrinsic planar Hall effect, *Phys. Rev. Lett.* **132**, 056301 (2024).
- <sup>16</sup> C. Zeng, S. Nandy, and S. Tewari, Fundamental relations for anomalous thermoelectric transport coefficients in the nonlinear regime, *Phys. Rev. Res.* **2**, 032066(R) (2020).
- <sup>17</sup> D.-K. Zhou, Z.-F. Zhang, X.-Q. Yu, Z.-G. Zhu, and G. Su, Fundamental distinction between intrinsic and extrinsic nonlinear thermal Hall effects, *Phys. Rev. B* **105**, L201103 (2022).
- <sup>18</sup> H. Varshney, K. Das, P. Bhalla, and A. Agarwal, Quantum kinetic theory of nonlinear thermal current, *Phys. Rev. B* **107**, 235419 (2023).
- <sup>19</sup> H. Varshney, R. Mukherjee, A. Kundu, and A. Agarwal, Intrinsic nonlinear thermal Hall transport of magnons: A quantum kinetic theory approach, *Phys. Rev. B* **108**, 165412 (2023).
- <sup>20</sup> Y.-F. Zhang, Z.-F. Zhang, Z.-G. Zhu, and G. Su, Second-order intrinsic Wiedemann-Franz law, *Phys. Rev. B* **111**, 165424(2025).
- <sup>21</sup> X.-Q. Yu, Z.-G. Zhu, J.-S. You, T. Low, and G. Su, Topological nonlinear anomalous Nernst effect in strained transition metal dichalcogenides, *Phys. Rev. B* **99**, 201410(R) (2019).
- <sup>22</sup> C. Zeng, S. Nandy, A. Taraphder, and S. Tewari, Nonlinear Nernst effect in bilayer WTe<sub>2</sub>, *Phys. Rev. B* **100**, 245102 (2019).
- <sup>23</sup> Y.-L. Wu, G.-H. Zhu, and X.-Q. Yu, Nonlinear anomalous nernst effect in strained graphene induced by trigonal warping, *Phys. Rev. B* **104**, 195427 (2021).
- <sup>24</sup> H. Varshney and A. Agarwal, Intrinsic nonlinear Nernst and Seebeck effect, *New J. Phys.* **27**, 083506 (2025).
- <sup>25</sup> H. Liu, H. Jiang, J. Li, Z. Zhang, X. C. Xie, P. He, J. Zhai, M. Zhang, and J. Shen, Nonlinear Nernst effect in trilayer graphene at zero magnetic field, *Nat. Nanotech.* **20**, 1221-1227 (2025).
- <sup>26</sup> Y. Gao and D. Xiao, Orbital magnetic quadrupole moment and nonlinear anomalous thermoelectric transport, *Phys. Rev. B* **98**, 060402(R) (2018).
- <sup>27</sup> X.-G. Ye, H. Liu, P.-F. Zhu, W.-Z. Xu, S. A. Yang, N. Shang, K. Liu, and Z.-M. Liao, Control over Berry curvature dipole with electric field in WTe<sub>2</sub>, *Phys. Rev. Lett.* **130**, 016301 (2023).
- <sup>28</sup> A. Bhattacharya and A. M. Black-Schaffer, Electric field induced second-order anomalous hall transport in unconventional Rashba systems, *Phys. Rev. B* **111**, L041202 (2025).
- <sup>29</sup> A. Mukherjee, B. Sanyal, A. M. Black-Schaffer, and A. Bhattacharya, Electric field controlled second-order anomalous hall effect in altermagnets, arXiv:2510.14899.
- <sup>30</sup> S. Korrapati, S. Nandy and S. Tewari, Electric field induced Berry curvature dipole and non-linear anomalous Hall effect in higher wave symmetric unconventional magnets, arXiv:2510.20237v1.
- <sup>31</sup> H. Li, M. Li, R.-C. Xiao, W. Liu, L. Wu, W. Gan, H. Han, X. Tang, C. Zhang, and J. Wang, Current induced second-order nonlinear Hall effect in bulk WTe<sub>2</sub>, *Appl. Phys. Lett.* **123**(16), 163102 (2023).
- <sup>32</sup> J. Yang, L. Wei, Y. Li, L. Chen, W. Niu, S. Wang, F. Li, P. Liu, S. Zhou, and Y. Pu, Electric field control of nonlinear Hall effect in the type-II Weyl semimetal TaIrTe<sub>4</sub>, *Appl. Phys. Lett.* **127**, 033102 (2025).
- <sup>33</sup> T. Nag, S. K. Das, C. Zeng, and S. Nandy, Third-order Hall effect in the surface states of a topological insulator, *Phys. Rev. B* **107**, 245141(2023).
- <sup>34</sup> Y. Gao, S. A. Yang, and Q. Niu, Field-induced positional shift of Bloch electrons and its dynamical implications, *Phys. Rev. Lett.* **112**, 166601 (2014).
- <sup>35</sup> S. Lai, H. Liu, Z. Zhang, J. Zhao, X. Feng, N. Wang, C. Tang, Y. Liu, K. S. Novoselov, S. A. Yang, and W.-B. Gao, Third-order nonlinear Hall effect induced by the Berry-connection polarizability tensor, *Nat. Nanotechnol.* **16**, 869 (2021).

<sup>36</sup> H. Liu, J. Zhao, Y.-X. Huang, W. Wu, X.-L. Sheng, C. Xiao, and S. A. Yang, Intrinsic second-order anomalous hall effect and its application in compensated antiferromagnets, *Phys. Rev. Lett.* **127**, 277202 (2021).

<sup>37</sup> H. Liu, J. Zhao, Y.-X. Huang, X. Feng, C. Xiao, W. Wu, S. Lai, W.-B. Gao, and S. A. Yang, Berry connection polarizability tensor and third-order Hall effect, *Phys. Rev. B* **105**, 045118 (2022).

<sup>38</sup> D. Xiao, W. Yao, and Q. Niu, Valley-contrasting physics in graphene: Magnetic moment and topological transport, *Phys. Rev. Lett.* **99**, 236809 (2007).

<sup>39</sup> A. H. Castro Neto, F. Guinea, N. M. R. Peres, K. S. Novoselov, and A. K. Geim, The electronic properties of graphene, *Rev. Mod. Phys.* **81**, 109 (2009).

<sup>40</sup> K. Das, K. Ghorai, D. Culcer, and A. Agarwal, Nonlinear valley hall effect, *Phys. Rev. Lett.* **132**, 096302 (2024).

<sup>41</sup> Ying-Li Wu, Jia-Liang Wan, and Xiao-Qin Yu, Intrinsic nonlinear valley Nernst effect in the strained bilayer graphene, *Phys. Rev. B* **112**, 144104 (2025).

<sup>42</sup> Y. Gao, Semiclassical dynamics and nonlinear charge current, *Frontiers of Physics*, **14**(3), 33404 (2019).